Total reflection of optical beams by weakly oscillating dielectric scatterers

Er'el Granot
Department of Electrical and Electronics Engineering, Ariel University, Ariel
(Received 24 October 2016; published 13 December 2016)

It is well known that in quantum mechanics a weak scatterer can act as a perfect reflector provided it oscillates at a specific frequency, which is close to that of the incident particles. This is a Fano resonance, in which case the propagating wave mode destructively interferes with the bound state. Due to the high frequencies of the optical domain, it is not possible to design an optical device, which is based on this effect. However, if the beam propagates in a narrow waveguide with conducting boundaries, then even a weak dielectric scatterer, which oscillates at the frequency difference between the optical frequency and the threshold frequency of the waveguide, can block the optical beam. This frequency difference can be *arbitrarily small*. A model for such a system is presented and solved exactly numerically without approximations. For a weak scatterer an approximate analytical expression is suggested for the point of perfect reflection. Finally, a physical realization is suggested. This effect can be used for controlling optical beams by submicron devices.

DOI: 10.1103/PhysRevA.94.063828

I. INTRODUCTION

Tunneling is a unique quantum phenomenon. Quantum particles can penetrate barriers, which are classically impenetrable (see, for example Refs. [1,2]). On the other hand, finite potential barriers cannot be perfect reflectors. Any finite width barrier has a nonzero transmission coefficient as well as a nonzero reflection coefficient. Even a δ-function potential, which has an infinite potential, cannot completely block quantum particles. The δ function can simulate a narrow potential since the integral over this potential is finite. Had it been infinite, it would have blocked the quantum particle, but any physical scatterer has a finite integral and therefore cannot have zero transmission (see, for example, [1–3]). However, in quantum mechanics there is a remarkable phenomenon: When a δ-function potential oscillates, and the incoming particle has a certain frequency, which is a little below the oscillating frequency, then the particle is totally reflected; i.e., the transmission coefficient vanishes [4–10]. It should be stressed that this is not an approximation. It is not that most of the quantum particles are reflected, but *all* of them are. A thorough and accurate analysis of the zeros and resonances in this quantum phenomenon can be found in Refs. [6,8].

The problem of tunneling in the presence of an oscillating potential received a lot of attention in the literature since it shed light on the enigmatic process of tunneling [11–20]. Moreover, this problem was also found useful for microelectronic devices driven by oscillating electric field [21–27] and even for biochemistry [27–33].

Harnessing this effect to the optical domain could be very useful in generating small-factor modulator as well as optical transistors. However, this peculiar quantum effect is absent in the optical domain. Besides the fact that the dispersion relation is different (linear instead of parabolic), it is technologically impossible to oscillate the refraction index at optical frequencies [34–36].

However, there is another perfect-reflection effect, which occurs in the quantum domain. It has been shown that when a quantum particle propagates in a narrow orifice, i.e., nanowire, and its energy is close to the orifice threshold energy, the particle can be reflected with probability 1 by hitting a point potential defect [37–39]. This effect occurs only at specific energy; however, it occurs for *any* point potential, no matter how weak. This effect was used to prove that, in the presence of *any* point defect, a universal conductance reduction of exactly e^2/h occurs [39].

It is the object of this paper to apply the waveguide geometry to the optical domain to change the relevant dispersion relation and to ease dramatically the requirement put on the refractive index's oscillations.

It should be stressed that the similarity between the two cases, namely, the stationary two-dimensional (2D) waveguide case [37–39] and the dynamic one-dimensional (1D) case [4–10] is not accidental. In both cases, the continuum interferes with a bound state, and Fano resonances appear [40] (for Fano resonances in a narrow orifice, see Ref. [41]; as a result of a dynamic breather, see Ref. [42]; and for an extensive review, see Ref. [43]). Therefore, the zero transmission effect is a well-known phenomenon. The unique aspect of the present work is that it occurs for optical beams, while the blocking scatterer oscillates at much lower frequencies.

As a consequence, this effect can be used in relatively simple optical devices. In particular, it may be incorporated in small-factor modulators, switches, and even frequency controlled optical transistors.

II. MOTIVATION

When a quantum particle propagates with frequency ω and hits a scatterer, which oscillates at frequency $\Omega \cong \omega$, it may lose frequency quanta Ω, and if the oscillating frequency is larger than the incoming particle's frequency, namely $\Omega > \omega$, the particle cannot propagate and is bound to be reflected. Clearly, in the optical domain the requirement $\Omega > \omega$ is unattainable. Usually $\Omega \ll \omega$, and therefore, such a scatterer has a negligible effect on the scattered particle.

However, when a photon propagates in a narrow waveguide with conducting boundaries, and its polarization is orthogonal to the waveguide's plane, then the propagating constant is

$$k = \sqrt{\left(\frac{n_0\omega}{c}\right)^2 - \left(\frac{\pi}{a}\right)^2}, \tag{1}$$

where a is the waveguide's width, n_0 is the refractive index, ω is the frequency, and c is the velocity of light. Then, in case $\frac{n_0\omega}{c} \cong \frac{\pi}{a}$, the difference between propagating and evanescent waves can be arbitrarily small. Even if the initial frequency is above the cutoff frequency, i.e.,

$$\frac{n_0\omega}{c} > \frac{\pi}{a}, \tag{2}$$

then after losing frequency quantum the frequency can be lower than the cutoff frequency,

$$\frac{n_0(\omega - \Omega)}{c} < \frac{\pi}{a}. \tag{3}$$

As a consequence the wave becomes evanescent and the transmission coefficient may vanish.

Clearly, (2) and (3) are not sufficient conditions for zero transmission coefficient. The requirement is much more subtle; however, they are a definitely necessary condition, and the waveguide makes them feasible.

III. THEORY AND MODEL

The system is illustrated in Fig. 1. A z-polarized electromagnetic (EM) wave propagates in the x direction, while being confined in the y direction to a waveguide, whose width is a.

The EM field wave equation reads

$$\left(\frac{\partial^2}{\partial x^2} + \frac{\partial^2}{\partial y^2}\right)\mathbf{E}(x,y,t) - \frac{n^2(x,y,t)}{c^2}\frac{\partial^2}{\partial t^2}\mathbf{E}(x,y,t) = 0, \tag{4}$$

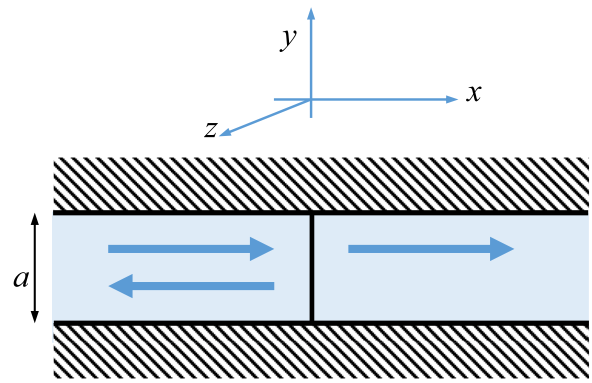

FIG. 1. System schematic: Dielectric waveguide with a narrow oscillating defect at $x = 0$.

where

$$\mathbf{E}(x,y,t) = \begin{cases} \hat{z}E(x,y,t) & 0 < y < a \\ 0 & \text{else} \end{cases}$$

is the polarized EM field and

$$n^2(x,t) = n_0^2 + w\left[\Delta n_1^2 + \Delta n^2 \cos(\Omega t)\right]\delta(x) \tag{5}$$

is the square of the refraction index. Therefore, the refraction index is constant along the waveguide except for the location of the oscillating scatterer at $x = 0$.

If the incident wave is confined to the first transverse mode then the generic solution can be written

$$\frac{\mathbf{E}(x,y,t)}{E_0} = \begin{cases} \sin\left(\frac{\pi y}{a}\right)\exp\left(ik_{1,0}x - i\omega_0 t\right) + \sum_{qm}\sin\left(\frac{q\pi y}{a}\right) r_{qm}\exp\left(-ik_{qm}x - i\omega_m t\right) & x < 0 \\ \sum_{qm}\sin\left(\frac{q\pi y}{a}\right) t_{qm}\exp\left(ik_{qm}x - i\omega_m t\right) & x > 0 \end{cases}, \tag{6}$$

where

$$\omega_m \equiv \omega + m\Omega,$$

$$k_{qm} \equiv \sqrt{\left(\frac{n_0\omega_m}{c}\right)^2 - \left(\frac{q\pi}{a}\right)^2}, \tag{7}$$

and the summation symbol indicates double summation: $\sum_{qm} \equiv \sum_{q=1}^{\infty}\sum_{m=-\infty}^{\infty}$.

However, since the scatterer has no transversal structure, it cannot scatter between transverse modes, and therefore (6) can be rewritten in a simpler form,

$$\frac{\mathbf{E}(x,y,t)}{E_0} = \begin{cases} \sin\left(\frac{\pi y}{a}\right)\left\{\exp\left(ik_0 x - i\omega_0 t\right) + \sum_m r_m \exp\left(-ik_m x - i\omega_m t\right)\right\} & x < 0 \\ \sin\left(\frac{\pi y}{a}\right)\sum_m t_m \exp\left(ik_m x - i\omega_m t\right) & x > 0 \end{cases}, \tag{8}$$

when

$$k_m \equiv \sqrt{\left(\frac{n_0\omega_m}{c}\right)^2 - \left(\frac{\pi}{a}\right)^2}; \tag{9}$$

i.e., $k_m = k_{1m}$.

After matching the solution on two sides of the oscillating scatterer, the following difference equation emerges:

$$\delta(m) + r_m = t_m \tag{10}$$

and

$$t_m\left(2ik_m + \frac{w\Delta n_1^2}{c^2}\omega_m^2\right) + \frac{w\Delta n^2}{2c^2}\left[t_{m+1}\omega_{m+1}^2 + t_{m-1}\omega_{m-1}^2\right] = 2ik_0\delta(m)m, \tag{11}$$

which can be rewritten in a simpler form,

$$\tau_m[\chi(m) - i\gamma] - i\delta[\tau_{m+1} + \tau_{m-1}]/2 = \delta(m), \tag{12}$$

where

$$\tau_m \equiv t_m \frac{\omega_m^2}{\omega_0^2}, \quad \gamma \equiv \frac{w\Delta n_1^2 \omega_0^2}{2c^2 k_0}, \quad \delta \equiv \frac{w\Delta n^2 \omega_0^2}{2c^2 k_0}, \quad \text{and}$$

$$\chi(m) \equiv \frac{\omega_0^2}{\omega_m^2}\frac{k_m}{k_0}. \tag{13}$$

The proximity to the cutoff frequency can be quantified by the following parameter:

$$Q \equiv \frac{\pi c}{a n_0 \omega_0}. \tag{14}$$

When $Q = 1$ the particle's initial frequency $\omega_0 = \omega$ is equal to the threshold energy,

$$\omega_c \equiv \frac{\pi c}{a n_0}. \tag{15}$$

Then, with this notation,

$$\chi(m) = \frac{\sqrt{(1 + m\Omega/\omega_0)^2 - Q^2}}{(1 + m\Omega/\omega_0)^2\sqrt{1 - Q^2}}. \tag{16}$$

When $\Omega \ll \omega$, then $\chi(m) \cong 1$, and therefore (12) can be approximated by

$$\tau_m(1 - i\gamma) - i\delta[\tau_{m+1} + \tau_{m-1}]/2 = \delta(m), \tag{17}$$

whose solution is

$$\tau_m \cong \frac{i}{\delta\sqrt{A^2 - 1}}(-A + \sqrt{A^2 - 1})^{|m|}, \tag{18}$$

where

$$A = \frac{(i + \gamma)}{\delta}, \tag{19}$$

when $\delta \ll 1$ (18) becomes

$$\tau_m \cong \frac{i}{\delta A}\left(-\frac{1}{2A}\right)^{|m|} = \frac{1}{1 - i\gamma}\left[-\frac{\delta}{2(i + \gamma)}\right]^{|m|}. \tag{20}$$

These solutions and their resemblance to the exact solution are presented in Fig. 2. A spatiotemporal presentation of a sample solution's intensity $|\mathbf{E}(x, y = a/2, t)/E_0|^2$ is presented in Fig. 3. In this regime, the oscillating frequency is very low, and therefore, one can adopt the approximation

$$k_m = k_0\sqrt{1 + 2m\omega\Omega\left(\frac{n_0}{c}\right)^2 \Big/ k_0^2} \cong k_0 + m\omega\Omega\left(\frac{n_0}{c}\right)^2 \Big/ k_0, \tag{21}$$

and, in fact the entire dynamics is governed by only three modes, $m = -1,0,1$. Therefore, the solution can be approximated by

$$E(x,y,t)/E_0$$
$$\cong \sin\left(\frac{\pi y}{a}\right)\left\{\exp(ik_0 x) - \frac{\exp(ik_0|x|)}{1 + i/\gamma} - i\frac{\delta\exp(ik_0|x|)}{(1 - i\gamma)^2}\right.$$
$$\left.\times\cos\left[\frac{\omega\Omega}{k_0}\left(\frac{n_0}{c}\right)^2 x + \Omega t\right]\right\}\exp(-i\omega_0 t). \tag{22}$$

A sample dynamics of such a (numerically exact) solution is presented in Fig. 3. The Ω oscillations are clearly shown in time. In the spatial domain there is a clear difference between the two half spaces ($x < 0$ and $x > 0$). In front of the scatterer ($x < 0$) the dominant wavelength is $2\pi/k_0$, while beyond the scatterer ($x > 0$) the dominant wavelength is $2\pi k_0/[\omega\Omega(n_0/c)^2]$, which is considerably larger.

Since there is only a single weak scatterer, then for most incoming energies the scattering is governed by these three modes; however, like in the quantum case, this behavior breaks down when the oscillating frequency approaches the spectral gap between the photons' frequency and the waveguide's cutoff frequency.

In Fig. 4 the transmission coefficient of the main mode is plotted as a function of the normalized oscillating frequency

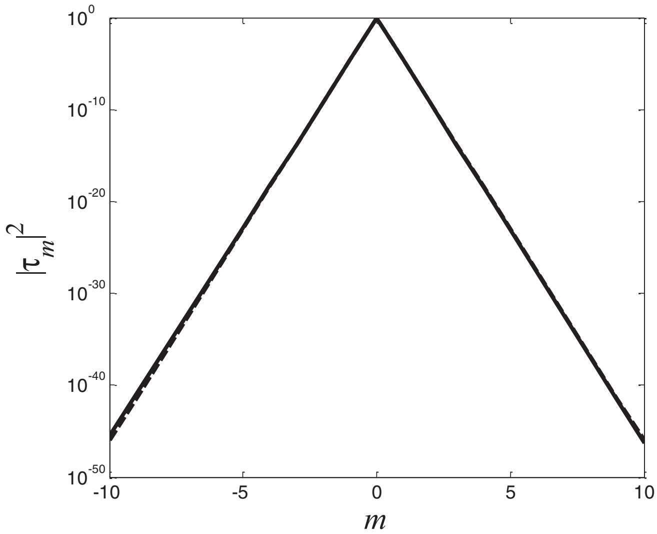

FIG. 2. The solution of the difference equation (12) for the parameters $Q = 0.8$, $\Omega/\omega = 0.01$, $\delta = 0.01$, $\gamma = 0.04$. The exact solution is presented by the solid curve and the approximation (18) is presented by the dashed curve.

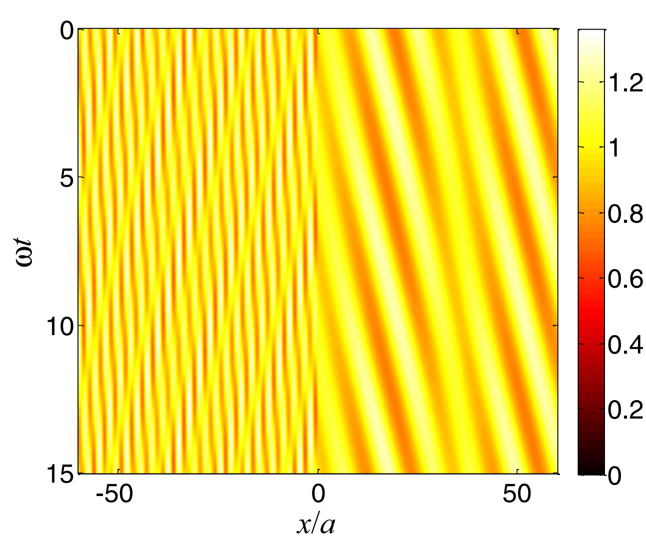

FIG. 3. A spatiotemporal presentation of the solution's intensity in the presence of a weak oscillating defect. The defect divides space into two regimes, which are clearly seen in this figure. In this case the parameters are $Q = 0.93$, $\delta = 0.1$, $\gamma = 0.04$, and $\Omega/\omega = 0.05$.

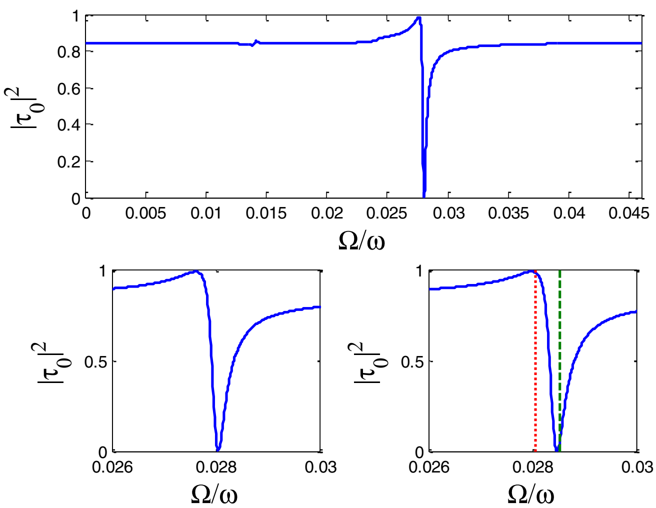

FIG. 4. The transmission coefficient of the main mode as a function of the normalized oscillating frequency. The upper panel represents the exact solution, the lower-left figure is a magnification of the transition region, and the right figure represents the approximate solution (24), with the approximate evaluation of the minimum frequency (dashed horizontal line) and maximum frequency (dotted horizontal line). In this case the parameters are $Q = 0.975\,68$, $\delta = 0.2$, and $\gamma = 0.4$.

Ω/ω. As can be seen (in the upper panel) when Ω/ω is just above the $1 - Q = 0.0243$ there is a dip (at $\Omega/\omega \cong 0.028$), in which τ_0 vanishes.

At this unique frequency, just as in the quantum counterpart, all higher modes vanish as well; i.e., $\tau_m = 0$ for $m \geqslant 0$. Again, it should be emphasized that this is not an approximation, but that the transmission coefficient is exactly zero.

Similarly, another peculiar point occurs a little below the vanishing point, where the transmission coefficient is equal to 1. In this case the scatterer is totally transparent (for similar behavior in the quantum case, see Refs. [6,8]).

To find the vanishing point from (12) we can neglect τ_{-3} and substitute $\tau_m = 0$ for $m \geqslant 0$, in which case the problem reduces to zeroing the determinant,

$$\begin{vmatrix} \chi(-1) - i\gamma & -i\delta/2 \\ -i\delta/2 & \chi(-2) - i\gamma \end{vmatrix} = 0. \tag{23}$$

When $Q \cong 1$ and $\frac{\Omega}{\omega_0}\frac{1}{(1-Q)} \cong 1$, then $\chi(m)$ can be approximated as

$$\chi(m) \cong \sqrt{1 + m\Omega/\omega_0(1 - Q^2)}. \tag{24}$$

This case is illustrated in the lower-right panel of Fig. 4. Under this approximation

$$\chi(-2) \cong i \quad \text{and} \quad \chi(-1) \cong i\sqrt{\frac{\Omega}{\omega_0}\frac{1}{(1-Q)} - 1}, \tag{25}$$

and therefore the oscillating frequency, for which the transmission coefficient vanishes, can be approximated by

$$\frac{\Omega_{\min}}{\omega_0} \cong (1 - Q)\left\{1 + \left[\frac{\delta^2}{4(1-\gamma)} + \gamma\right]^2\right\}. \tag{26}$$

This evaluation of the minimum's location is presented by the horizontal dashed line in the right-lower panel of Fig. 4.

Similarly, the frequency, for which the transmission coefficient is 1, can be evaluated by substituting $\tau_0 = 1$, $\tau_m = 0$ for $m \geqslant 1$, and neglecting τ_{-3}. The result is

$$\frac{\Omega_{\max}}{\omega_0} \cong (1 - Q)\left\{1 + \left[\gamma - \frac{\delta^2}{4\gamma}\frac{(1-2\gamma)}{(1-\gamma)}\right]^2\right\}. \tag{27}$$

This evaluation of the maximum's location is presented by the horizontal dotted line in the right-lower panel in Fig. 4.

Thus, the spectral width of the transmission's transition from 1 to 0 can be evaluated by

$$\frac{\Omega_{\max} - \Omega_{\min}}{\omega_0} \cong (1 - Q)\frac{\delta^2}{2}, \tag{28}$$

which surprisingly is independent of γ. This estimation is much more accurate than both (26) and (27).

In Fig. 5 the spatiotemporal dynamic of the intensity at the zero transmission point is illustrated.

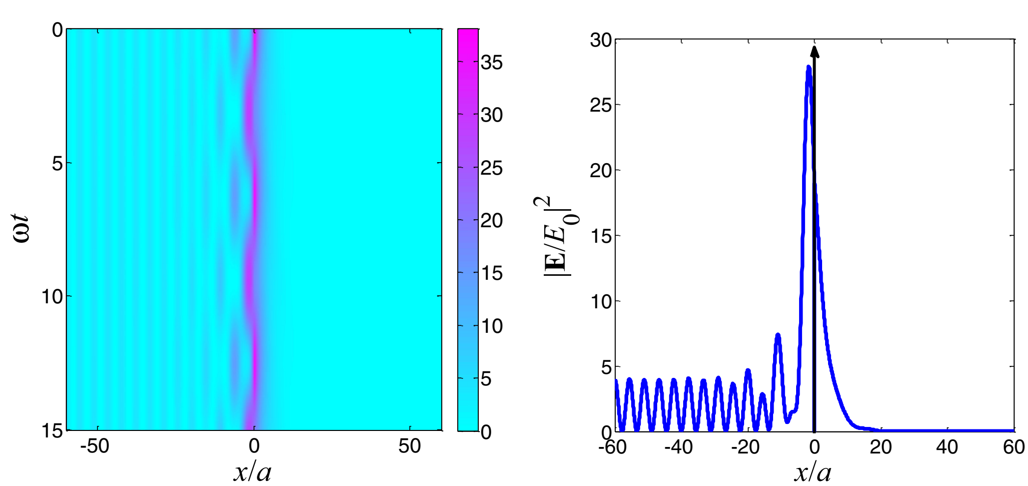

FIG. 5. The spatiotemporal dynamics of the zero transmission point (left) and the spatial distribution of the intensity for $\omega t = 15$ (right). The simulation parameters are $Q = 0.975\,68$, $\delta = 0.4$, $\gamma = 0.2$, and $\Omega/\omega = 0.0256$.

At this point all energy (or photons) is reflected; however, like a resonant scenario there is an accumulation of photons at the vicinity of the defect. The weaker the defect (δ), the larger is the accumulation. This is illustrated by the value of the intensity on the defect. This value oscillates with the oscillation frequency,

$$|\mathbf{E}(x=0,y,t)/E_0|^2 \cong \sin^2\left(\frac{\pi y}{a}\right)\frac{4}{\delta^2}\left[1+\frac{\delta}{(1-\gamma)}\cos(\Omega t)\right]. \tag{29}$$

IV. PHYSICAL ESTIMATION AND REALIZATION

A possible realization is a $LiNbO_3$ waveguide (with refraction indices $n_o = 2.238$ and $n_e = 2.159$) of width $a = 0.335\,\mu$m and metallic boundaries. When a standard tunable laser for the optical C band [36] is used as the optical source, it can transmit the wavelength $\lambda = 1.5\,\mu$m with the bandwidth $\Delta\lambda = 0.1$ nm. Therefore, $1 - Q \cong 6.7 \times 10^{-5}$. The oscillating defect can then be realized by applying an electric field on the defect's location (by a narrow capacitor plate, whose width is $w = 0.1\,\mu$m). Let the applied alternating voltage be $V = 10$ V; then (see Ref. [35])

$$\delta \cong \frac{w}{a}\frac{n_e^3}{2} r_{33} V k \frac{1}{2}\sqrt{\frac{\lambda}{2\Delta\lambda}} \cong 0.05, \tag{30}$$

where for this case $r_{33} = 30\,\text{pm V}^{-1}$ is the Pockels coefficient. Two scenarios are possible: If the optical axis remains parallel to the z axis even outside the defect zone, then $\gamma = 0$; otherwise, if outside the defect zone the optical axis is parallel to the y axis, then $\gamma \cong 0.63$.

The former scenario is presented in Fig. 6. In this case the evaluation of the minimum is very accurate:

$$f_{\min} = \frac{\omega_0}{2\pi}(1-Q)\left(1+\frac{\delta^4}{16}\right) = 13.4\,\text{GHz}. \tag{31}$$

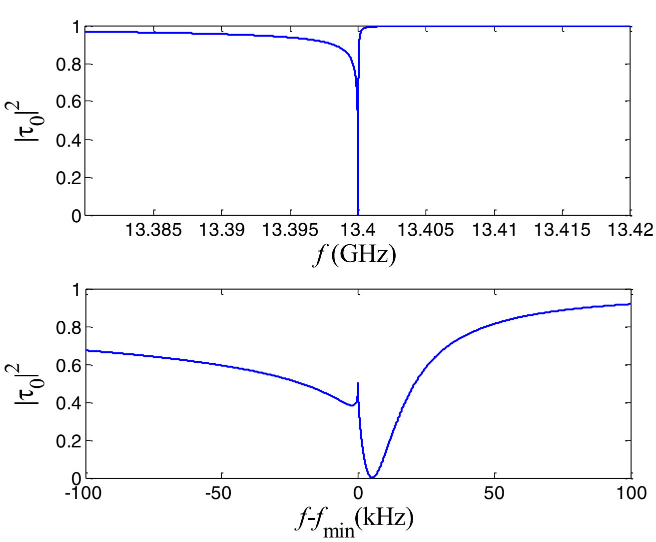

FIG. 6. The transmission of the main mode as a function of the oscillating frequency $f = \Omega/2\pi$ for the first scenario. The lower panel is a magnification of the transition zone ($f_{\min} = 13.4$ GHz).

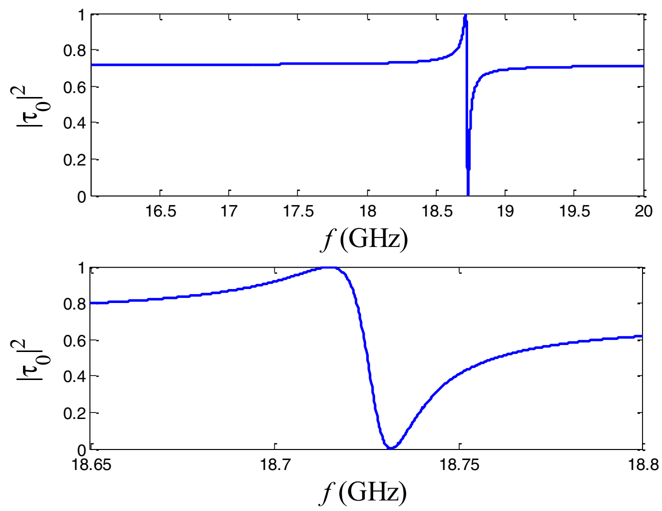

FIG. 7. Same as Fig. 6 but for the second scenario.

The inaccuracy is only about a few kilohertz. This frequency is easily achieved with optical communications equipment. Since $\gamma = 0$ the transmission coefficient never gets to the value 1.

In the latter case since γ is not a small parameter the approximation is

$$f_{\min} \cong \frac{\omega_0}{2\pi}(1-Q)\left\{1+\left[\frac{\delta^2}{4(1-\gamma)}+\gamma\right]^2\right\} \cong 19.4\,\text{GHz}, \tag{32}$$

which is a less accurate evaluation of the real value $f_{\min} \cong 18.73$ GHz (see Fig. 7).

However, the transition

$$f_{\max} - f_{\min} \cong \pi(1-Q)\frac{\delta^2}{\omega_0} = 16.75\,\text{MHz} \tag{33}$$

is an excellent approximation.

V. CONCLUSIONS AND SUMMARY

The purpose of this paper was to harness waveguide topology to mimic the quantum effect of perfect reflection in the optical domain. In the quantum domain an oscillating point potential can totally reflect a scattering particle. However, this effect requires a square dispersion relation and also requires that the oscillating frequency would be close to the incoming particle's frequency. These requirements are essential, since they ensure that by losing frequency quanta the incoming wave turns from a propagating mode to an evanescent one. Both of these requirements are unattainable in the ordinary optical world, where the dispersion relation is linear and the optical frequencies are considerably larger than any oscillating reflector (excluding nonlinear effects, of course).

We demonstrate that by using waveguide geometry these requirements become feasible in the optical world. We solve such a model exactly numerically and demonstrate that it can be easily detected in common optical communications equipment.

This effect can be utilized to control optical beams by submicron devices, and therefore can be used for small-form-factor modulators and even optical transistors.

ACKNOWLEDGMENT

I would like to thank Prof. Eli Eisenberg who informed me about the zero-transmission case in the quantum domain some twenty years ago.

[1] D. Bohm, *Quantum Theory* (Dover Publications, New York, 1989).
[2] E. Merzbacher, *Quantum Mechanics* (Wiley, New York, 1970).
[3] E. Granot, Transmission coefficient for a point scatterer at specific energies is affected by the presence of the scatterer but independent of the scatterer's characteristics, Phys. Rev. B **71**, 035407 (2005).
[4] E. Cota, J. V. Jose, and F. Rojas, Electronic transmission through time-periodic oscillating barriers, Nanostruct. Mater. **3**, 349 (1993).
[5] P. F. Bagwell and R. K. Lake, Resonances in transmission through an oscillating barrier, Phys. Rev. B **46**, 15329 (1992).
[6] W. Li and L. E. Reichl, Floquet scattering through a time-periodic potential, Phys. Rev. B **60**, 15732 (1999).
[7] D. S. Saraga and M. Sassoli-de-Bianchi, On the one-dimensional scattering by time-periodic potentials: General theory and application to two specific models, Helv. Phys. Acta **70**, 751 (1997).
[8] D. F. Martinez and L. E. Reichl, Transmission properties of the oscillating δ-function potential, Phys. Rev. B **64**, 245315 (2001).
[9] D. L. Haavig and R. Reifenberger, Dynamic transmission and reflection phenomena for a time-dependent rectangular potential, Phys. Rev. B **26**, 6408 (1982).
[10] W. Cai, P. Hu, T. F. Zheng, B. Yudanin, and M. Lax, Resonance of the one-dimensional electron transmission above a quantum well with dissipation, Phys. Rev. B **41**, 3513 (1990).
[11] M. Büttiker and R. Landauer, Traversal Time for Tunneling, Phys. Rev. Lett. **49**, 1739 (1982).
[12] M. Büttiker and R. Landauer, Traversal time for tunneling, Phys. Scr. **32**, 429 (1985).
[13] J. A. Støvneng and E. H. Hauge, The Büttiker-Landauer model generalized, J. Stat. Phys. **57**, 841 (1989).
[14] M. Wagner, Quenching of resonant transmission through an oscillating quantum well, Phys. Rev. B **49**, 16544 (1994).
[15] M. Wagner, Strongly Driven Quantum Wells: An Analytical Solution to the Time-Dependent Schrödinger Equation, Phys. Rev. Lett. **76**, 4010 (1996).
[16] M. Wagner, Can photon-assisted tunneling be observed in single barriers? Phys. Status Solidi B **204**, 382 (1997).
[17] M. Y. Azbel, Eigenstate Assisted Activation, Phys. Rev. Lett. **68**, 98 (1992).
[18] M. Y. Azbel, Elevator resonance activation, Europhys. Lett. **18**, 537 (1992).
[19] E. Granot, Selected elevation in quantum tunneling, Europhys. Lett. **61**, 817 (2003).
[20] G. Zangwil and E. Granot, Eigenstate suppressed activation, Physica B **461**, 140 (2015).
[21] M. Wagner, Photon-assisted transmission through an oscillating quantum well: A transfer-matrix approach to coherent destruction of tunneling, Phys. Rev. A **51**, 798 (1995).
[22] M. Wagner and W. Zwerger, Characteristic scaling parameters for tunneling in strong time-dependent electric fields, Phys. Rev. B **55**, R10217 (1997).
[23] M. Wagner, Tunneling spectrum of a strongly driven double-well diode, Phys. Rev. B **57**, 11899 (1998).
[24] S. Datta and M. P. Anantram, Steady-state transport in mesoscopic systems illuminated by alternating fields, Phys. Rev. B **45**, 13761 (1992).
[25] P. Johansson and G. Wendin, Tunneling through a double-barrier structure irradiated by infrared radiation, Phys. Rev. B **46**, 1451 (1992).
[26] H. C. Liu, Analytical model of high-frequency resonant tunneling: The first-order ac current response, Phys. Rev. B **43**, 12538 (1991).
[27] E. Granot and G. Zangwill, Dynamic resonant tunneling, in *Research Advances in Quantum Dynamics*, edited by P. Bracken (InTech, Rijeka, Croatia, 2016), Chap. 3, pp. 55–78.
[28] H. B. Gray and J. R. Winkler, Electron tunneling through proteins, Q. Rev. Biophys. **36**, 341 (2003).
[29] S. Lloyd, Quantum coherence in biological systems, J. Phys.: Conf. Ser. **302**, 012037 (2011).
[30] L. Turin, A spectroscopic mechanism for primary olfactory reception, Chem. Senses **21**, 773 (1996).
[31] G. M. Dyson, The scientific basis of odour, Chem. Ind. **57**, 647 (1938).
[32] J. C. Brookes, F. Hartoutsiou, A. P. Horsfield, and A. M. Stoneham, Could Humans Recognize Odor by Phonon Assisted Tunneling? Phys. Rev. Lett. **98**, 038101 (2007).
[33] N. Pavlicek, I. Swart, J. Niedenfuhr, G. Meyer, and J. Repp, Symmetry Dependence of Vibration-Assisted Tunneling, Phys. Rev. Lett. **110**, 136101 (2013).
[34] J.-M. Liu, *Photonic Devices* (Cambridge University Press, Cambridge, 2005).
[35] G. P. Agrawal, *Fiber-Optic Communication Systems* (John Wiley & Sons, New York, 2002).
[36] B. E. A. Saleh and M. C. Teich, *Fundamentals of Photonics* (Wiley-Interscience Publications, New York, 1991).
[37] P. F. Bagwell, Evanescent modes and scattering in quasi-one-dimensional wires, Phys. Rev. B **41**, 10354 (1990).
[38] P. F. Bagwell, Solution of Dyson's equation in a quasi-1D wire, J. Phys.: Condens. Matter **2**, 6179 (1990).
[39] E. Granot, Universal conductance reduction in a quantum wire, Europhys. Lett. **68**, 860 (2004).
[40] U. Fano, Effects of configuration interaction on intensities and phase shifts, Phys. Rev. **124**, 1866 (1961).
[41] Y. S. Joe, A. M. Satanin, and C. S. Kim, Classical analogy of Fano resonances, Phys. Scr. **74**, 259 (2006).
[42] S. Flach, A. E. Miroshnichenko, V. Fleurov, and M. V. Fistul, Fano Resonances with Discrete Breathers, Phys. Rev. Lett. **90**, 084101 (2003).
[43] A. E. Miroshnichenko, S. Flach, and Y. S. Kivshar, Fano resonances in nanoscale structures, Rev. Mod. Phys. **82**, 2257 (2010).